

# New Approach to Strong Correlation: Twisting Hubbard into the Orbital Hatsugai-Kohmoto Model

Peizhi Mai<sup>1</sup>, Jinchao Zhao<sup>1</sup>, Gaurav Tenkila<sup>1</sup>, Nico A. Hackner<sup>1</sup>, Dhruv Kush<sup>1</sup>, Derek Pan<sup>1</sup>, Philip W. Phillips<sup>1,†</sup>

<sup>1</sup>*Department of Physics and Institute of Condensed Matter Theory,  
University of Illinois at Urbana-Champaign, Urbana, IL 61801, USA*

(Dated: October 2023)

Based on the surprising observation that all the correlation functions in the local-in-momentum space Hatsugai-Kohmoto (HK) model fall off exponentially with distance, we show that the  $N_\alpha$ -orbital extension has a fundamental connection with the Hubbard model. Namely, for  $N_\alpha$ -orbitals on each of the  $N$   $\mathbf{k}$ -points and dynamics between the orbital degrees of freedom, the  $N_\alpha$ -orbital HK model is equivalent to covering the Brillouin zone with  $N/N_\alpha$  Hubbard clusters each containing  $N_\alpha$ -sites all connected via twisted boundary conditions. The thermodynamic limit arises from the  $\mathbf{k}$ -state starting point of the HK model. While the Hubbard model necessarily results when  $N_\alpha = N$ , we show that already at  $N_\alpha = 2, 4$ , standard results for the Hubbard model emerge, such as the onset of an insulating state regardless of the strength of the interactions, double occupancy, dynamical spectral weight transfer, charge neutral excitations leading to the algebraic temperature dependence of the specific heat, all with a fraction of the computational time of more advanced cluster methods and making it possible to obtain analytical insights. Consequently, the  $N_\alpha$ -orbital HK model offers a new tool for strongly correlated quantum matter.

## INTRODUCTION

The paradigmatic model for strong correlations in quantum matter is that of electrons hopping on a lattice between nearest neighbors but paying the energy cost  $U$  anytime they doubly occupy the same site. Naively, the energy eigenstates of this model would seem to be ordered with respect to the number of doubly occupied sites. However, this fails because the potential and kinetic terms do not commute. As a result, electrons can lower their energy by hopping to sites with single occupancy. It is for this reason that this simple model remains unsolved in any dimension exceeding unity, thereby remaining a grand challenge as it is the gold standard for Mott physics in the cuprates. The state-of-the-art remains quantum Monte Carlo[1–5], density matrix renormalization group[1–3, 6] and dynamical mean-field theory (DMFT)[7–9] and its cluster versions such as cellular DMFT[10, 11] and the dynamical cluster approximation (DCA)[12–15] which have all been useful in unveiling the properties of the Hubbard model including the pseudogap[12, 16–19], superconductivity[3, 12] and transport[9, 20, 21] in the strange metal regime.

A natural question arises: Is there an alternative? The more tractable formulation of Mott physics is the Hatsugai-Kohmoto (HK) model[22] which we referred to as the band HK model in the following. It has a repulsion between any two electrons with opposite spin that doubly occupy the same momentum state. Consequently, the doubly occupied band steadily increases in energy as the repulsion increases resulting in an insulating state in a half-filled band when the interaction strength exceeds the bandwidth. In this model, double occupancy is the organizing principle for the ordering of the eigenstates. Clearly then, this is a gross simplification of the Hubbard model stemming from the locality in momentum space (long-range interactions in real space) and generating a macroscopic spin degeneracy in the singly occupied sector. In essence, the solvability of band HK rests on the commutativity of the potential and kinetic energy terms. Can such

non-commutativity be put back in systematically, thereby reducing the difference with the Hubbard model, without giving up on exact solvability?

We show here that this can be done. Our work shows that two rather seemingly disparate approaches, the momentum-space or band HK model and the exact diagonalization of small Hubbard clusters share a fundamental link. That band HK and the local physics of a Hubbard cluster might be related because all the  $n$ -point correlation functions in the band HK model fall off exponentially. Consequently, the seeming non-locality of this model is actually a ruse. Further demonstration of locality is that the Mott transition to the insulating state proceeds via the depletion of the quasiparticle peak at zero energy as in single-site DMFT[7], an artifact of single-impurity physics. To build in the non-commutativity of the energy terms in the Hamiltonian, we show that the orbital[23–25] HK model suffices. Here the Mott transition at 1/2-filling resembles the accepted scenario[12] in two dimensions (2D) that no conducting states survive for any non-zero value of  $U$ . As a result of the non-commutativity, the orbital HK model exhibits dynamical mixing[26, 27] across the Mott gap, namely dynamical spectral weight transfer (DSWT), a key non-trivial feature of the Hubbard model. But unlike Hubbard, exact solvability is not sacrificed. It is the DSWT that makes it possible to establish an exact mapping between the two models.

## LOCAL CORRELATIONS

The starting point for our analysis is Fig. 1a which shows that although the HK model has all-to-all interactions, the 2-point correlator falls off exponentially. The same is true for the 4-point and all higher correlation functions. This is significant because Wightman’s reconstruction theorem[28] ensures that if all the  $n$ -point functions are local, then so is the theory. The question arises, why does a model admit non-local interactions at the level of the Hamiltonian but exhibit purely local

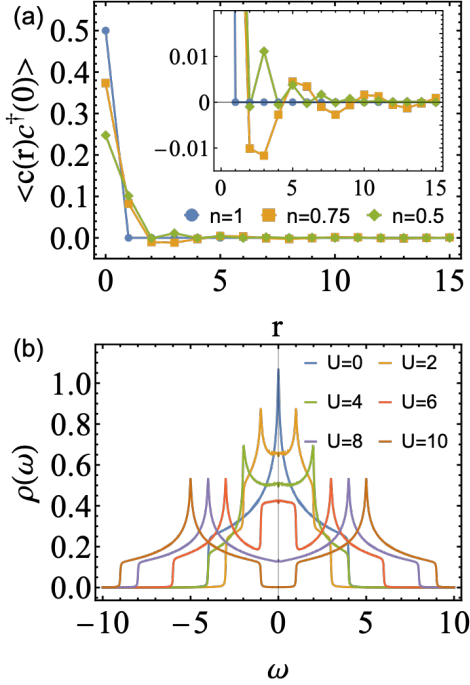


FIG. 1: (a) 2-point correlator showing the absence of long-range correlations in the band HK model at different densities despite the all-to-all nature of the interactions in real space with  $U/t = 10$  and  $\beta = 50/t$ . Here  $r = r_x = r_y$ . (b) The density of states under different  $U$  displaying Mott transition at the half-filled band HK model with  $\beta = 200/t$ .

correlations? To gain insight into this, we plot in Fig. 1b the density of states for various  $U$  across the Mott transition of the half-filled band HK model, which interestingly has never been computed. Here the Mott transition to the insulating state proceeds via depletion of the density of states at the central peak at  $\omega = 0$  as in the standard single-site DMFT model[7]. This is telling and consistent with the exponential fall-off of the  $n$ -point correlators: all the physics is local regardless of the non-local nature of the Hamiltonian. This can be understood simply. The Hamiltonian for the band HK model is identical in form to the atomic limit[23] of the Hubbard model with the band index  $\mathbf{k}$  replacing the site index  $\mathbf{i}$ . A more precise statement will be made later when we complete the mapping to the full Hubbard model.

### ORBITAL HK

However, just like DMFT, the basic band HK model does not capture the full Hubbard physics. As pointed out previously[23], band HK can be generalized to include multiple orbitals per  $\mathbf{k}$ -state as is necessary for the adaption of this model to QAH and QSH topological models, all of which have 2 atoms per unit cell[24, 25]. Such a change produces qualitatively new physics as the hybridization between the orbitals lifts[23] the thermodynamic degeneracy of the band HK

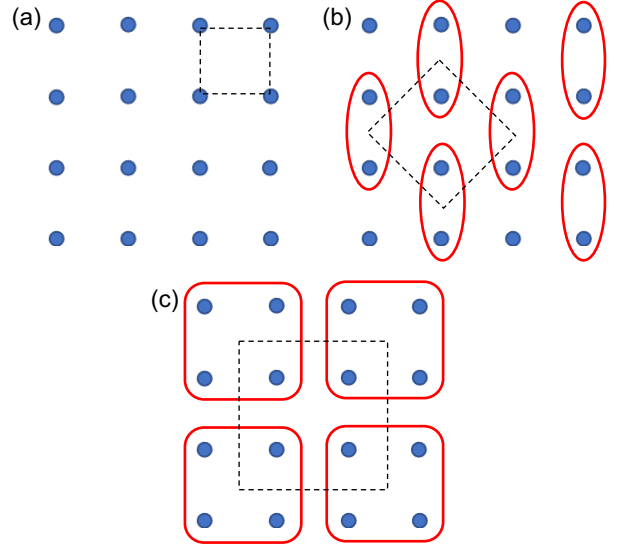


FIG. 2: Scheme of the orbital unit cell (encircled by red lines) and lattice (dashed lines) for the orbital HK model: a) 1-orbital= band HK model. b) The 2-orbital HK model leads to a doubling of the unit cell size and consequently halves the Brillouin zone (BZ). c) The 4-orbital HK model results in a quadrupling of the unit cell size and reduces the BZ to one-quarter of its original size.

model. Inspired by that, we adopt an orbital HK model to capture the strongly correlated dynamical mixing in a simple square lattice by redefining a set of lattice sites as orbitals. The most general version of this model is given by

$$H_{\text{OHK}} = \sum_{\mathbf{k}, \alpha, \alpha', \sigma} g_{\alpha, \alpha'}(\mathbf{k}) c_{\mathbf{k}\alpha\sigma}^\dagger c_{\mathbf{k}\alpha'\sigma} - \mu \sum_{\mathbf{k}, \alpha} n_{\mathbf{k}\alpha, \sigma} + \sum_{\mathbf{k}, \alpha, \alpha'} U_{\alpha, \alpha'} n_{\mathbf{k}\alpha\uparrow} n_{\mathbf{k}\alpha'\downarrow}, \quad (1)$$

where  $g(\mathbf{k})$  is the dispersion matrix determined by the underlying lattice hopping process and orbital setup,  $\alpha(\alpha')$  is the orbital index and  $\sigma$  is the spin. The computational time is governed by the diagonalization of the Fock-space matrix of dimension  $4^{N_\alpha} \times 4^{N_\alpha}$ . The redefinition of lattice sites as  $N_\alpha$  orbitals is depicted in Fig. 2. Explicitly shown are the 2 and 4-orbital cases in Fig. 2(b) and (c) respectively. Note that the orbital interactions are all local in the orbital basis while the hoppings occur among different orbitals, hence representing the built-in Hubbard physics for an  $N_\alpha$ -site cluster[23]. Also, we have included inter-orbital interactions in the most general case while our simulations shown below are only for the intra-orbital case. To see the effect of just a 2-orbital extension, look no further than the corresponding density of states at half-filling in Fig. 3a. Any non-zero  $U$  is sufficient to eliminate the metallic state producing a vanishing of the density of states at zero energy. Also of note is the narrowing of the bands which is completely absent in the band HK model. No qualitatively new physics appears in the Mott transition of the 4-orbital HK model at half-filling (Fig. 3b). These results are similar to those from state-of-the-art cluster versions of

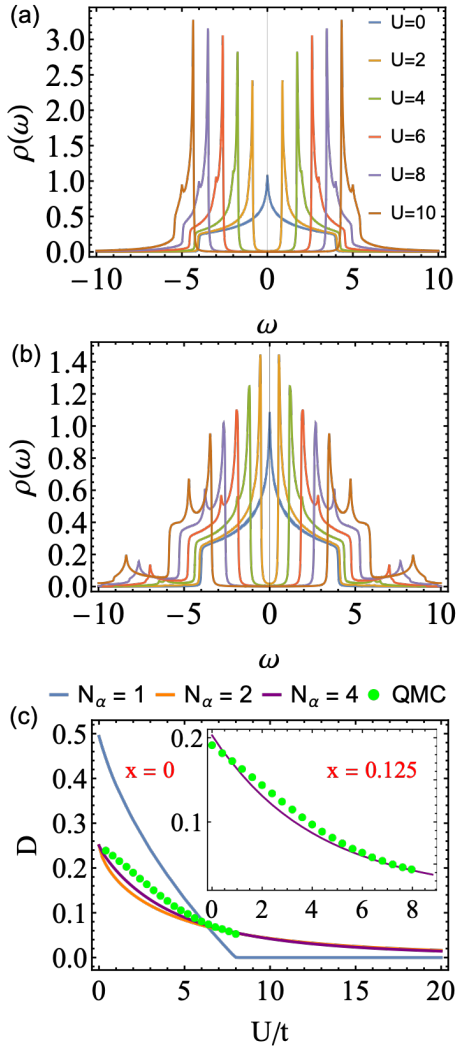


FIG. 3: Density of states representing Mott transition at half-filling of the (a) 2-orbital and (b) 4-orbital HK model (sharing the same legend), and (c) double occupancy at half-filling ( $x = 0$ ) as a function of  $U$  for the orbital HK model with various  $N_\alpha$ . The green dots are from auxiliary-field quantum Monte Carlo (QMC) simulations on the 2D Hubbard model[29]. The inset of panel (c) compares the 4-orbital HK and QMC results[29] at 1/8-hole-doping ( $x = 0.125$ ).

DMFT methods[7, 12]. We also calculate the double occupancy defined as

$$D = \frac{1}{N} \sum_{\mathbf{k},\alpha} \langle n_{\mathbf{k}\alpha\uparrow} n_{\mathbf{k}\alpha\downarrow} \rangle \quad (2)$$

directly related to the interaction energy. Consider the stark difference between the non-interacting limits of the band and orbital HK models in terms of double occupancy. Regardless of the model, in the non-interacting limit, the expression for  $D$  factorizes

$$D_{\text{non-int}} = \frac{1}{N} \sum_{\mathbf{k},\alpha} \langle n_{\mathbf{k}\alpha\uparrow} \rangle \langle n_{\mathbf{k}\alpha\downarrow} \rangle. \quad (3)$$

For the band HK model, half the Brillouin zone (BZ) is doubly occupied. That is,  $\langle n_{\mathbf{k}\alpha\sigma} \rangle = 1$  if occupied and zero otherwise. Consequently,  $D_{\text{non-int}} = 1/2$ . On the other hand, for the orbital model,  $\langle n_{\mathbf{k}\alpha\sigma} \rangle = \langle n_{\mathbf{k}\beta\sigma} \rangle$  for all  $\alpha \neq \beta$  by rotational symmetry. In addition,  $\langle n_{\mathbf{k}\alpha\sigma} \rangle = 1/2$  in the reduced Brillouin zone is not unity as in the starting band HK model. As a result, we find that for the orbital HK model,  $D_{\text{non-int}} = 1/4$ . Note that this result is identical to the non-interacting limit of the Hubbard model and underscores how drastically band HK differs from its orbital counterpart. The plots for the  $D$  show this dramatic difference. In band HK,  $D$  decreases steadily from  $1/2$  and vanishes for  $U > W$ . However, in orbital HK model,  $D$ , starting at  $1/4$ , just tapers asymptotically as  $U$  increases. Note also the rapid convergence between the 2 and 4-orbital cases which matches perfectly with state-of-the-art auxiliary-field quantum Monte Carlo simulations (QMC) on the Hubbard model[29]. The inset also shows the double occupancy of the 4-orbital HK model at 1/8-hole-doping ( $x = 0.125$ ) and its comparison with QMC simulations[29]. Once again, the agreement is remarkable underscoring that orbital HK converges rapidly to Hubbard physics. Additionally, the computational cost for solving the 4-orbital HK model is considerably lower, both in terms of algorithm development (40 lines of Mathematica) and actual code execution, when compared to QMC or cluster-type DMFT simulations on the Hubbard model. Most crucially, the orbital HK model is more amenable to analytical calculations, an aspect we intend to explore in future studies.

The fact that the double occupancy only vanishes asymptotically as  $U$  increases in the orbital HK model implies the presence of dynamical mixing between the upper and lower Mott sub-bands. This arises entirely from the non-commutativity[26, 27, 30] of the kinetic and potential energy and appears as  $t/U$  corrections to the low-energy spectral weight (LESW). In the atomic limit, the LESW is strictly  $2x$  because each hole can be occupied by a spin-up or spin-down electron. Any dynamical corrections to this necessarily generate double occupancy and hence increase the LESW strictly defined as

$$\Lambda(x) \equiv \text{LESW} = \int_0^{\omega_g} N(\omega) d\omega. \quad (4)$$

In Fig. (4), we compare the LESW of the 4-orbital HK model with Fig. (3) of Ref. [26]. There is no qualitative difference with exact diagonalization on the (1D) Hubbard model[26, 27]. Both increase faster than  $2x$ . The semiconductor (dashed line) and Fermi liquid (dashed-dotted) results are shown for comparison. As the occupied part of the lower band has a weight  $1 - x$ , the total weight in the lower band now exceeds  $1 + x$ . As only  $1 + x$  electrons can occupy the lower band, dynamical spectral weight transfer (DSWT) defined as  $\Lambda(x) - 2x$  and plotted in Fig. (4b) implies[31] that the spectral weight in the lower band cannot be exhausted by counting electrons alone. Fig. (4b) is quantitatively in agreement with the Hubbard model (Fig. (4) of Ref. [26]), the only difference being the maximum value which for 4-orbital HK

is 0.15 whereas it is 0.23 for the (1D) Hubbard result. Consequently, that the LESW in the orbital HK model increases faster than  $2x$  is a profoundly non-trivial result as no analytically solvable model has ever been formulated to capture this feature of the Hubbard model.

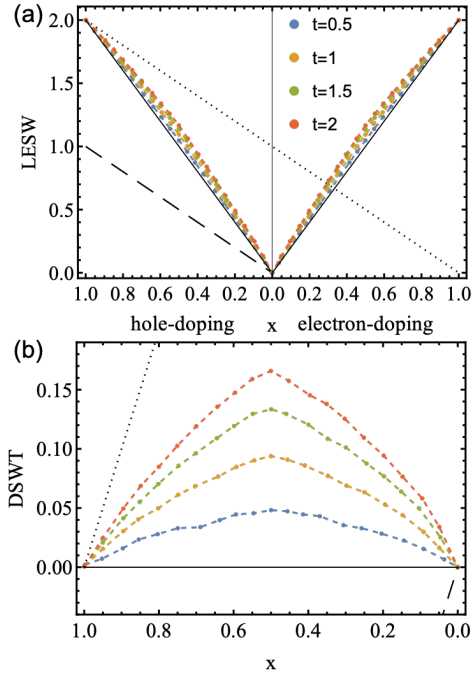


FIG. 4: LESW and DSWT in the exact solution of the 4-orbital HK model ( $U = 20$ ) for the hopping parameters shown in panels (a) and (b) respectively. The solid line shown with slope  $2x$  is the band HK or atomic Hubbard result. The dashed and dotted lines depict the semiconductor and Fermi liquid results respectively. Note, there is no qualitative difference with the exact diagonalization results for the Hubbard model[26, 27]. As  $t/U$  increases, so does the DSWT.

All of these results point to a fundamental connection with the Hubbard model. Fig. 2 contains the essential idea. Grouping the  $N$  lattice sites (or  $\mathbf{k}$ -points) into cells (Fig. 2(a-c)) with  $N_\alpha$  orbitals reduces the number of unit cells (or  $\mathbf{k}$ -points) to  $N/N_\alpha$ . That is, the high momenta are systematically being removed. Each cell in momentum space now contains the exact information of the  $N_\alpha$ -site Hubbard model. For example,  $N_\alpha = 2$  signifies that the orbital basis contains the information of the Hubbard dimer which has a non-degenerate ground state, and hence the spurious  $2^N$  spin degeneracy of the band-HK model is removed. In addition to hybridization between orbitals in each cell, the cells are also connected in terms of hopping and interactions. For  $N_\alpha = 4$ , we show the explicit connection between the cells. The matrix  $g(\mathbf{k})$ , representing the hopping connectivities in Fig. 2c, is given by

$$\begin{pmatrix} 0 & \varepsilon_{tx} & \varepsilon_{ty} & \varepsilon_{t'} \\ \varepsilon_{tx} & 0 & \varepsilon_{t'} & \varepsilon_{ty} \\ \varepsilon_{ty} & \varepsilon_{t'} & 0 & \varepsilon_{tx} \\ \varepsilon_{t'} & \varepsilon_{ty} & \varepsilon_{tx} & 0 \end{pmatrix} \quad (5)$$

for the 4-orbital case, with  $\varepsilon_{tx} = -2t \cos k_x$ ,  $\varepsilon_{ty} = -2t \cos k_y$  and  $\varepsilon_{t'} = -4t' \cos k_x \cos k_y$ , identical in form to that in the  $2 \times 2$  Hubbard cluster with twisted boundary conditions (TBC) [32] where  $\alpha$  is replaced with the site index  $i$  and  $k_x = \theta_x$  and  $k_y = \theta_y$  where  $\theta_x$  and  $\theta_y$  define the TBC. Besides, TBC gives local-in-momentum interactions in the reduced BZ which is exactly the interaction term in Eq. (1). For any  $N_\alpha < N$ , the orbital HK model corresponds to a  $N/N_\alpha$  copies of  $N_\alpha$ -site Hubbard clusters all connected by TBC. The matrix that determines the TBC is purely local as it is determined by the dynamics. Hence, orbital HK is purely local in the reduced Brillouin zone regardless of the number of orbitals used, even  $N_\alpha = 1$  corresponding to band HK whose locality is illustrated in Fig. 1. In this case, the TBC matrix is simply  $\varepsilon_{\mathbf{k}}$ . This exact mapping is a surprise and offers a new way of interpreting exact diagonalization with TBC. The most general statement is as follows. *Theorem:* The orbital HK model is equivalent to covering the Brillouin zone with  $N/N_\alpha$  Hubbard clusters each containing  $N_\alpha$ -sites all connected via TBC. Clearly, the  $N$ -site Hubbard model results when  $N_\alpha = N$ . Loosely, the  $N/N_\alpha$  identical copies throughout the Brillouin zone can be thought of as replica copies.

Aside from DSWT, the orbital HK model also exhibits a pseudogap in the density of states. Shown in Fig. 5 is the density of states for the 4-orbital HK model with (Fig. 5(a,c)) and without (Fig. 5(b,d)) the next-nearest-neighbor hopping,  $t'$ . Fig. 5(a) shows a suppression of the density of states at the chemical potential ( $\rho(\omega = 0) \lesssim 0.1$ ) in the underdoped region with  $t' = -0.25$  when  $U \geq W$  ( $W = 8t$  is the bare bandwidth), indicative of a pseudogap in the absence of superconducting order. The complete tracking of the density of states at zero frequency in Fig. 5(c) displays the trend that as  $U$  increases, the pseudo-gap region appears and extends to higher hole-doped density. In contrast, when  $t' = 0$ , the pseudo-gap suppression does not arise until  $U \gg W$ , as shown in Fig. 5(b,d). These observations are consistent with a recent study[32] on a  $2 \times 2$  Hubbard cluster with TBC. Finally, we compute the heat capacity of the 4-orbital HK model at half-filling shown in Fig. 6. Most noticeable is the two-peak structure at  $U > W$  representing a demarcation of the charge and spin degrees of freedom into high and low-temperature regimes, respectively, consistent with QMC simulations on the Hubbard model [33, 34]. Also at half-filling, we find a near-crossing of the heat capacity curves as a function of  $U$  at a temperature intermediate between the spin and charge excitations. The Maxwell relations governing the entropy dictate[35] such a crossing. Since there is no sign-problem restriction, we can access the low-temperature heat capacity exactly. As we show in Fig. 6(b), the low-temperature heat capacity data follow a power-law increase detailed in the supplement. While such algebraic growth might seem counter-intuitive for a Mott insulator, the first-excited state is charge neutral[36, 37] as shown in the supplement. Such charge-neutral excitations determine the low-T behavior of the specific heat.

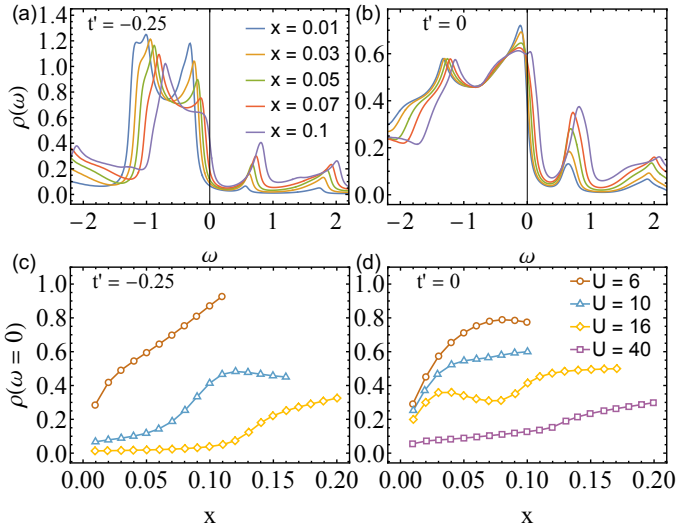


FIG. 5: Density of states at varying hole-doped densities with (a) and without (b) the next-nearest-neighbor hopping  $t'$  for the 4-orbital HK model ( $U/t = 10, \beta = 30/t$ ). Panel (a) and (b) share the same legend. Only for  $t' \neq 0$  is  $\rho(\omega)$  suppressed at zero frequency in the under-doped region, thereby indicating a pseudogap. Panel (c) and (d) show  $\rho(\omega = 0)$  with  $t' = -0.25$  and  $0$  respectively, as a function of hole-doped density under various  $U$ .

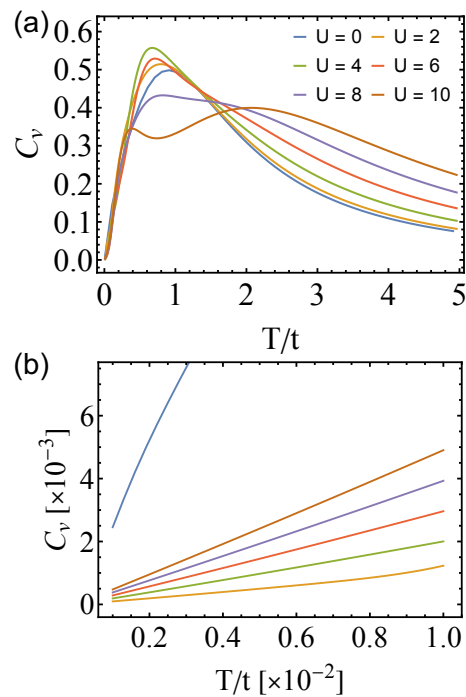


FIG. 6: Heat capacity of the half-filled 4-orbital HK model with various  $U$  at (a) high and (b) low temperatures. Both panels share the same legend.

## CONCLUDING REMARKS

We have shown here that orbital HK offers a powerful analytical tool for treating Mott physics described by the Hubbard model. While the agreement with Hubbard is expected in the large orbital number limit, already at  $N_\alpha = 2, 4$ , we find spot-on agreement with Hubbard for double occupancy at half-filling and 1/8-hole-doping as Fig. (3c) attests. This is not a surprise. After all, we have shown that HK represents a fixed point[38, 39] for Mott physics in which not even Hubbard is a relevant perturbation. The fixed point obtains because HK contains the most relevant interaction with scaling dimension  $-2$  of a Fermi liquid. The large negative scaling dimension stems from the single momentum integration. Adding orbitals to each  $\mathbf{k}$ -point does not lead to further momentum integrations as such decorations of each  $\mathbf{k}$ -point just appear as discrete summations. What the orbital content does add is non-commutativity between the kinetic and potential energy terms, thereby pushing it closer to the Hubbard model. Five manifestations of this non-commutativity stand out: 1) absence of a quasiparticle peak in the density of states at the Mott transition in agreement with standard Hubbard results[4, 5, 12], 2) the appearance of DSWT, 3) near-perfect quantitative agreement (see Fig. (3c)) with the QMC calculations on the Hubbard model for double occupancy that asymptotes to zero as  $U$  increases, 4) a pseudogap in the density of states, and 5) separation of spin and charge excitations in the heat capacity into low and high-temperature regimes. As all of this physics is present in the Hubbard model, we conclude the orbital HK model is an effective simulator of Mott physics exemplified by the Hubbard model. This connection is apparent because the orbital extension is equivalent to replicas of finite Hubbard clusters covering the Brillouin zone all connected via TBC. Given the simplicity and cost-effective nature of our approach, orbital HK represents a new computational tool for strongly correlated Mott physics.

**Acknowledgements** We thank Shiwei Zhang for sending us his double occupancy data that is plotted in Fig. 3 (green dots) and George Sawatzky for a helpful e-mail exchange. This work was supported by the Center for Quantum Sensing and Quantum Materials, a DOE Energy Frontier Research Center, grant DE-SC0021238 (P. M. and P. W. P.). PWP also acknowledges NSF DMR-2111379 for partial funding of the HK work which led to these results.

---

- [1] B.-X. Zheng, C.-M. Chung, P. Corboz, G. Ehlers, M.-P. Qin, R. M. Noack, H. Shi, S. R. White, S. Zhang, and G. K.-L. Chan, *Science* **358**, 1155 (2017).
- [2] E. W. Huang, C. B. Mendl, H.-C. Jiang, B. Moritz, and T. P. Devereaux, *npj Quantum Materials* **3**, 22 (2018).
- [3] M. Qin, C.-M. Chung, H. Shi, E. Vitali, C. Hubig, U. Schollwöck, S. R. White, and S. Zhang (Simons Collaboration on the Many-Electron Problem), *Phys. Rev. X* **10**, 031016 (2020), URL <https://link.aps.org/doi/10.1103/>

PhysRevX.10.031016.

[4] M. Qin, H. Shi, and S. Zhang, Phys. Rev. B **94**, 085103 (2016), URL <https://link.aps.org/doi/10.1103/PhysRevB.94.085103>.

[5] J. P. F. LeBlanc, A. E. Antipov, F. Becca, I. W. Bulik, G. K.-L. Chan, C.-M. Chung, Y. Deng, M. Ferrero, T. M. Henderson, C. A. Jiménez-Hoyos, et al. (Simons Collaboration on the Many-Electron Problem), Phys. Rev. X **5**, 041041 (2015), URL <https://link.aps.org/doi/10.1103/PhysRevX.5.041041>.

[6] H.-C. Jiang and S. A. Kivelson, Proceedings of the National Academy of Sciences **119**, e2109406119 (2022).

[7] A. Georges, G. Kotliar, W. Krauth, and M. J. Rozenberg, Reviews of Modern Physics **68**, 13 (1996).

[8] W. Xu, K. Haule, and G. Kotliar, Phys. Rev. Lett. **111**, 036401 (2013), URL <https://link.aps.org/doi/10.1103/PhysRevLett.111.036401>.

[9] X. Deng, J. Mravlje, R. Žitko, M. Ferrero, G. Kotliar, and A. Georges, Phys. Rev. Lett. **110**, 086401 (2013), URL <https://link.aps.org/doi/10.1103/PhysRevLett.110.086401>.

[10] H. Park, K. Haule, and G. Kotliar, Phys. Rev. Lett. **101**, 186403 (2008), URL <https://link.aps.org/doi/10.1103/PhysRevLett.101.186403>.

[11] S. S. Kancharla, B. Kyung, D. Sénéchal, M. Civelli, M. Capone, G. Kotliar, and A.-M. S. Tremblay, Phys. Rev. B **77**, 184516 (2008), URL <https://link.aps.org/doi/10.1103/PhysRevB.77.184516>.

[12] T. Maier, M. Jarrell, T. Pruschke, and M. H. Hettler, Rev. Mod. Phys. **77**, 1027 (2005), URL <https://link.aps.org/doi/10.1103/RevModPhys.77.1027>.

[13] P. Mai, S. Karakuzu, G. Balduzzi, S. Johnston, and T. A. Maier, Proceedings of the National Academy of Sciences **119**, e2112806119 (2022).

[14] P. Mai, N. S. Nichols, S. Karakuzu, F. Bao, A. Del Maestro, T. A. Maier, and S. Johnston, Nature Communications **14**, 2889 (2023).

[15] P. Werner, E. Gull, O. Parcollet, and A. J. Millis, Phys. Rev. B **80**, 045120 (2009), URL <https://link.aps.org/doi/10.1103/PhysRevB.80.045120>.

[16] T. D. Stanescu and G. Kotliar, Phys. Rev. B **74**, 125110 (2006), URL <https://link.aps.org/doi/10.1103/PhysRevB.74.125110>.

[17] M. Ferrero, P. S. Cornaglia, L. De Leo, O. Parcollet, G. Kotliar, and A. Georges, Phys. Rev. B **80**, 064501 (2009), URL <https://link.aps.org/doi/10.1103/PhysRevB.80.064501>.

[18] W. Wu, M. S. Scheurer, S. Chatterjee, S. Sachdev, A. Georges, and M. Ferrero, Phys. Rev. X **8**, 021048 (2018), URL <https://link.aps.org/doi/10.1103/PhysRevX.8.021048>.

[19] E. Gull, A. J. Millis, and O. Parcollet, p. 1 (2012), URL [http://inis.iaea.org/search/search.aspx?orig\\_q=RN:48038267](http://inis.iaea.org/search/search.aspx?orig_q=RN:48038267).

[20] E. W. Huang, R. Sheppard, B. Moritz, and T. P. Devereaux, Science **366**, 987 (2019).

[21] P. T. Brown, D. Mitra, E. Guardado-Sánchez, R. Nourafkan, A. Reymbaut, C.-D. Hébert, S. Bergeron, A.-M. S. Tremblay, J. Kokalj, D. A. Huse, et al., Science **363**, 379 (2019).

[22] Y. Hatsugai and M. Kohmoto, Journal of the Physical Society of Japan **61**, 2056 (1992), <https://doi.org/10.1143/JPSJ.61.2056>, URL <https://doi.org/10.1143/JPSJ.61.2056>.

[23] D. Manning-Coe and B. Bradlyn, Phys. Rev. B **108**, 165136 (2023), URL <https://link.aps.org/doi/10.1103/>PhysRevB.108.165136.

[24] P. Mai, B. E. Feldman, and P. W. Phillips, Phys. Rev. Res. **5**, 013162 (2023), URL <https://link.aps.org/doi/10.1103/PhysRevResearch.5.013162>.

[25] P. Mai, J. Zhao, B. E. Feldman, and P. W. Phillips, Nature Communications **14**, 5999 (2023), URL <https://doi.org/10.1038/s41467-023-41465-6>.

[26] M. B. J. Meinders, H. Eskes, and G. A. Sawatzky, Phys. Rev. B **48**, 3916 (1993).

[27] H. Eskes, M. B. J. Meinders, and G. A. Sawatzky, Phys. Rev. Lett. **67**, 1035 (1991), URL <https://link.aps.org/doi/10.1103/PhysRevLett.67.1035>.

[28] A. S. Wightman, Phys. Rev. **101**, 860 (1956), URL <https://link.aps.org/doi/10.1103/PhysRev.101.860>.

[29] H. Xu, H. Shi, E. Vitali, M. Qin, and S. Zhang (2024), unpublished.

[30] A. B. Harris and R. V. Lange, Phys. Rev. **157**, 295 (1967), URL <https://link.aps.org/doi/10.1103/PhysRev.157.295>.

[31] P. Phillips, Rev. Mod. Phys. **82**, 1719 (2010), URL <https://link.aps.org/doi/10.1103/RevModPhys.82.1719>.

[32] E. W. Huang, arXiv e-prints arXiv:2010.12601 (2020), 2010.12601.

[33] D. Duffy and A. Moreo, Phys. Rev. B **55**, 12918 (1997), URL <https://link.aps.org/doi/10.1103/PhysRevB.55.12918>.

[34] W. O. Wang, J. K. Ding, B. Moritz, E. W. Huang, and T. P. Devereaux, Phys. Rev. B **105**, L161103 (2022), URL <https://link.aps.org/doi/10.1103/PhysRevB.105.L161103>.

[35] D. Vollhardt, Phys. Rev. Lett. **78**, 1307 (1997), URL <https://link.aps.org/doi/10.1103/PhysRevLett.78.1307>.

[36] P. Mai, J. Zhao, T. A. Maier, B. Bradlyn, and P. W. Phillips, *Topological phase transition without single-particle-gap closing in strongly correlated systems* (2024), 2401.01402.

[37] J. Zhao, P. Mai, B. Bradlyn, and P. Phillips, Phys. Rev. Lett. **131**, 106601 (2023), URL <https://link.aps.org/doi/10.1103/PhysRevLett.131.106601>.

[38] J. Zhao, G. La Nave, and P. W. Phillips, Phys. Rev. B **108**, 165135 (2023), URL <https://link.aps.org/doi/10.1103/PhysRevB.108.165135>.

[39] E. W. Huang, G. L. Nave, and P. W. Phillips, Nature Physics **18**, 511 (2022), URL <https://doi.org/10.1038%2Fs41567-022-01529-8>.

# New Approach to Strong Correlation: Twisting Hubbard into the Orbital Hatsugai-Kohmoto Model: supplemental material

Peizhi Mai<sup>1</sup>, Jinchao Zhao<sup>1</sup>, Gaurav Tenkila<sup>1</sup>, Nico A. Hackner<sup>1</sup>, Dhruv Kush<sup>1</sup>, Derek Pan<sup>1</sup>, Philip W. Phillips<sup>1,†</sup>

<sup>1</sup>*Department of Physics and Institute of Condensed Matter Theory,  
University of Illinois at Urbana-Champaign, Urbana, IL 61801, USA*

## MOTT INSULATOR HEAT CAPACITY

A drastic difference between the single band HK model and a multi-orbital HK model is the energy gap between the ground state and the first excited state. Unlike the band HK model, the gap for multi-orbital HK model closes at a surface of points in the Brillouin zone where  $\varepsilon(k)$  vanishes. Here  $\varepsilon(k)$  is the lowest eigenvalue of the non-interacting Hamiltonian. Since the ground state and the first excited state have the same occupation numbers, the excitation is charge neutral and thus the system remains an insulator. Around this surface, the gap is proportional to

$$E_k^1 - E_k^0 = \frac{1}{2} \left( -U + \sqrt{U^2 + 16\varepsilon(k)^2} \right) \approx \frac{4\varepsilon(k)^2}{U}. \quad (1)$$

This behavior is universal in both  $N_\alpha = 2, 4$  orbital HK models. From now on we focus on the  $N_\alpha = 2$  case. The first excitation energy has a degeneracy  $d > 1$ . If we set  $\mu = U/2$ , we may ignore all the other excited states that are at least  $U/2$  above them. In the low-temperature regime  $\beta U/2 \gg 1$ , the total energy simplifies to

$$\begin{aligned} E(T) &\approx \sum_k \left( \frac{de^{-\beta E_k^1}}{Z} E_k^1 + \frac{e^{-\beta E_k^0}}{Z} E_k^0 \right) \\ &= \sum_k E_k^0 + \sum_k \frac{de^{-\beta E_k^1}}{Z} (E_k^1 - E_k^0) \\ &\approx E(0) + \sum_k \left( \frac{de^{-\beta \frac{4\varepsilon(k)^2}{U}}}{de^{-\beta \frac{4\varepsilon(k)^2}{U}} + 1} \frac{4\varepsilon(k)^2}{U} \right) \\ &= E(0) + \int d\varepsilon D(\varepsilon) \frac{d}{d + e^{\frac{4\beta\varepsilon^2}{U}}} \frac{4\varepsilon^2}{U}, \end{aligned} \quad (2)$$

where  $D(\varepsilon)$  is the density of states in terms of the lowest eigenvalue  $\varepsilon$  of the non-interacting Hamiltonian. At low temperature  $\beta t^2 \gg U$ , the integrand decays quickly as a function of  $\varepsilon$ . Thus if  $D(\varepsilon)$  does not vanish or have any singularity at  $\varepsilon = 0$ , we have

$$\begin{aligned} E(T) &\approx E(0) + D(0) \frac{\sqrt{U}}{2} \int dx \frac{dx^2}{d + e^{\beta x^2}} \\ &= E(0) - D(0) \frac{\sqrt{U}}{2} \frac{\sqrt{\pi}}{2} \text{Li}_{3/2}(-d) (k_B T)^{3/2}, \end{aligned} \quad (3)$$

where  $\text{Li}_n(z)$  is the polylogarithmic function and  $\text{Li}_{3/2}(-d) < 0$  when  $d > 0$ . Thus, the heat capacity becomes

$$C_v = -\frac{3\sqrt{\pi}}{8} \text{Li}_{3/2}(-d) D(0) k_B \sqrt{U k_B T}. \quad (4)$$

For the case when  $D(\varepsilon) \propto \varepsilon^\lambda$ , we have

$$\begin{aligned} E(T) - E(0) &\propto \int dx \frac{x^{2+\lambda}}{d + e^{\beta x^2}} \\ &\propto -\Gamma\left(\frac{3+\lambda}{2}\right) \text{Li}_{(3+\lambda)/2}(-d) (k_B T)^{(3+\lambda)/2}, \end{aligned} \quad (5)$$

By taking the temperature derivative, we obtain a  $T^{(1+\lambda)/2}$  dependence for  $C_v$ . This power law dependence on  $T$  surfaces from the charge-neutral excitation gap in the Mott insulating state, which is absent in band HK or trivial insulators which have an inverse exponential  $\exp(-\Delta/T)$  dependence instead. This behavior can be observed in the heat capacity of the  $N_\alpha = 1, 2, 4$  orbital HK model in Fig. 1.

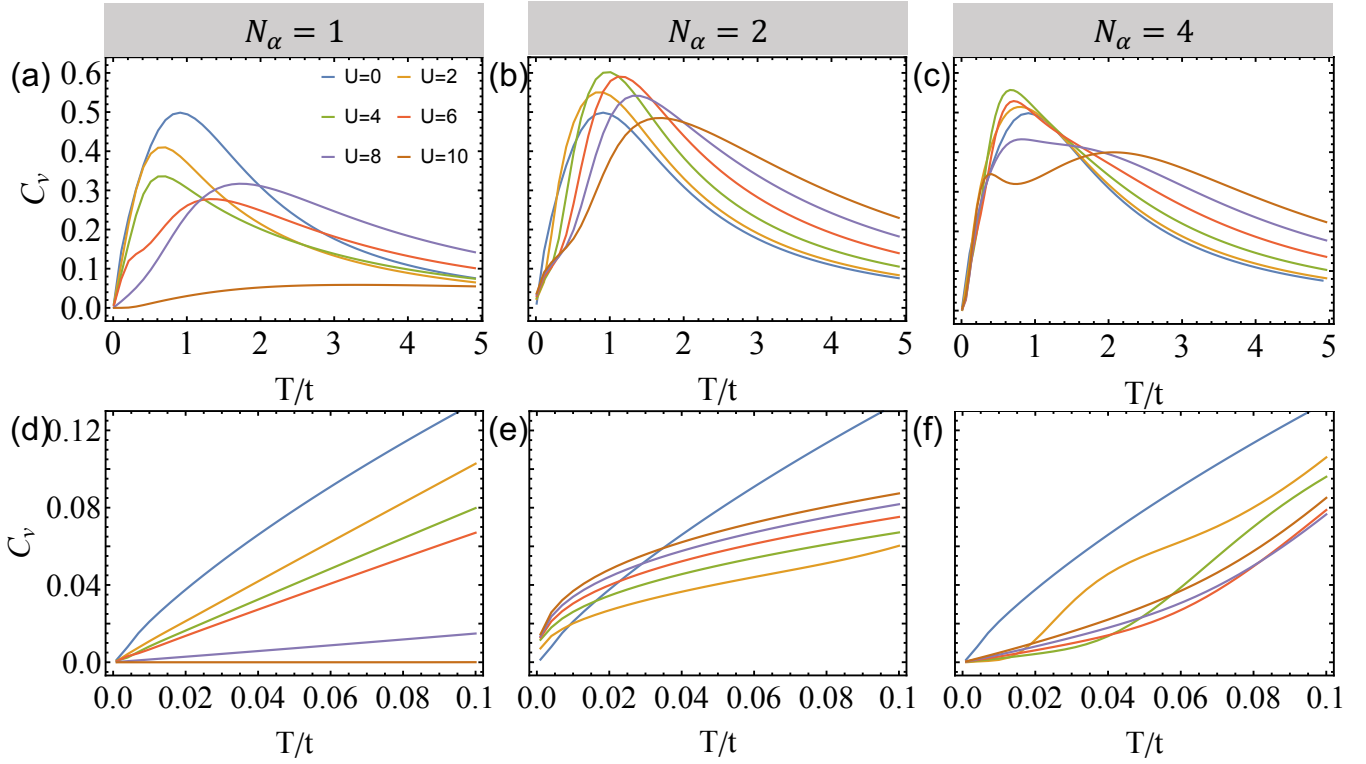


FIG. 1: Heat capacity for orbital-HK models with different number of orbitals  $N_\alpha = 1, 2, 4$  as labelled. Panels (a-c) are for high temperature, while panels (d-f) are for low temperatures.